Available online at www.sciencedirect.com
SCIENCE DIRECT®
International Journal of Heat and Mass Transfer 49 (2006) 4220–4230
International Journal of HEAT and MASS TRANSFER
www.elsevier.com/locate/ijhmt

The effect of tube diameter on vertical two-phase flow regimes in small tubes

L. Chen [a], Y.S. Tian [b], T.G. Karayiannis [a,*]

[a] School of Engineering and Design, Brunel University, West London, Uxbridge, Middlesex UB8 3PH, UK
[b] Aspentech Inc., 90 Milton Park, Abington, Oxfordshire OX14 4RY, UK

Received 5 July 2005
Available online 5 June 2006

Abstract

Flow boiling flow patterns in four circular tubes with internal diameters of 1.10, 2.01, 2.88 and 4.26 mm were investigated in the present project. The experiments were conducted in vertical upward two-phase flow using R134a as the working fluid. The observed flow patterns include dispersed bubble, bubbly, confined bubble, slug, churn, annular and mist flow. The flow characteristics in the 2.88 and 4.26 mm tubes are similar to those typically described in normal size tubes. The smaller diameter tubes, 1.10 and 2.01 mm, exhibit strong "small tube characteristics" as described in earlier studies. The sketched flow maps show that the transition boundaries of slug-churn and churn-annular depend strongly on diameter. On the contrary, the dispersed bubble to churn and bubbly to slug boundaries are less affected. The transition boundaries are compared with existing models for normal size tubes showing poor agreement.

Keywords: Flow patterns; Two-phase flow; Small diameter; Vertical

1. Introduction

The literature review carried out as part of this project revealed that there are a number of vague statements and discrepant results in the reported studies of two-phase flow regimes in small channels, which need further experimental work and theoretical investigation. To start with, the classification of normal, small and microchannels is not as yet well defined. Currently, the lack of general agreement on this issue makes the comparison between the experiments difficult, especially when using different fluids or at different experimental conditions. Engineers used to regard tube diameters in the order of centimetre and millimetre as normal and small-scale tubes, respectively. Now many researchers think the criterion ought to be based on the combination of channel size and fluid thermo-hydraulic properties rather than only on channel dimension. Kew and Cornwell [1] reported that two-phase flow exhibits different flow and heat transfer characteristics when the confinement number, $Co = (\sigma/\Delta\rho g D^2)^{1/2}$, is greater than 0.5. For instance, isolated bubbles prevail when $Co > 0.5$ and form a typical flow regime in small tubes, i.e. confined bubble flow. Brauner and Moalem-Maron [2] recommended Eötvös number, defined as $E\ddot{o} = (2\pi)^2\sigma/\Delta\rho g D^2$, as the criterion indicating confinement effects. They stated that surface tension dominates when $E\ddot{o} > 1$ and this marks the boundary for small passages. Triplett et al. [3] found that stratified flow became impossible when $E\ddot{o} > 100$ in their experiments indicating size effects. Akbar et al. [4] summarized the previous studies and concluded that the buoyancy effect can be negligible when the Bond number, $Bo = (\Delta\rho g D^2/\sigma)^{1/2}$, is less than 0.3 for which condition the flow regimes are insensitive to the channel orientation. In fact, all classification numbers, Co, $E\ddot{o}$ and Bo, consider the effect of fluid density, surface tension and channel size on two-phase flow. Table 1 illustrates the different results given by the above three criteria, i.e. the size of a tube that indicates deviation from normal size behaviour. The

* Corresponding author.
E-mail addresses: william.tian@aspentech.com (Y.S. Tian), tassos.karayiannis@brunel.ac.uk (T.G. Karayiannis).

0017-9310/$ - see front matter © 2006 Elsevier Ltd. All rights reserved.
doi:10.1016/j.ijheatmasstransfer.2006.03.025

Nomenclature

Bo	Bond number $\left[\sqrt{D^2 g(\rho_l - \rho_g)/\sigma}\right]$
Co	Confinement number $\left[\sqrt{\sigma/D^2 g(\rho_l - \rho_g)}\right]$
D	tube diameter, m
Eö	Eötvös number $[(2\pi)^2 Co^2]$
g	gravitational acceleration, m/s^2
u	velocity, m/s
We	Weber number $[\rho D u^2/\sigma]$

Greek symbols

ρ	density, kg/m^3
σ	surface tension, N/m

Subscripts

g	saturated gas/vapour
gs	based on superficial gas velocity
l	saturated liquid
ls	based on superficial liquid velocity

Table 1
The different criteria for small tubes

Parameters	Air/water	R134a		
Pressure (MPa)	0.10	0.60	1.00	1.40
Temperature (°C)	25.0	21.6	39.4	52.5
Surface tension	7.20E−02	8.39E−03	6.15E−03	4.61E−03
Gas density	1.185	29.04	49.06	70.7
Liquid density	997.0	1218.2	1148.3	1090.2
Gravitational acceleration	9.81	9.81	9.81	9.81
	Critical diameter (mm)			
Criterion based on $Eö = 1$	17.1	5.3	4.7	4.3
Criterion based on $Co = 0.5$	5.4	1.7	1.5	1.4
Criterion based on $Eö = 100$	1.71	0.53	0.47	0.43
Criterion based on $Bo = 0.3$	0.81	0.25	0.23	0.20

discrepancy is quite large especially if $Eö = 1$ is included. For example, as seen in the table, for the air/water mixture the criteria give a range from 0.81 to 17.1 mm. Note that the diameter corresponding to $Co = 0.5$ is 6.66 times that based on $Bo = 0.3$. Similarly the diameter is proportional to $Eö^{-1/2}$ so changing the criterion $Eö = 100$ to $Eö = 1$ increase the critical diameter by a factor of 10. Therefore, the need for further work to clarify and conclude on the classification of normal and small size tubes is obvious. The distinction between small diameter channels, mini-channels and microchannels based on heat transfer results, is not clearly established in the literature, Kandlikar [5]. He reviewed the developments and application of flow boiling in channels and summed up that: 3 mm may be the lower limit for the hydraulic diameters of the conventional evaporator tubes; channels employing hydraulic diameter between 200 and 3 mm maybe referred to as minichannels; tubes with 10–200 μm hydraulic diameter could be considered as microchannels. This is of course a general classification and further verification and adoption maybe needed.

In addition to the above, there is also inconsistency on the identification of flow patterns. Some flow maps sketched by different researchers may be dissimilar even though they used similar tubes under similar conditions. Fig. 1 compares the vertical upward flow maps by Oya [6], Barnea et al. [7], Fukano and Kariyasaki [8], and Mishima and Hibiki [9]. The disagreements are obvious. For example, large differences exist at the transition boundaries of dispersed bubble (or bubble) flow to intermittent flow and the transition boundary of intermittent to annular flow predicted by Barnea et al. and the rest of the researchers. Furthermore, the flow pattern descriptions presented by different researchers show variations. Oya preferred a detail classification. He reported simple bubble, granular-lumpy bubble, simple slug, fish-scale type slug, piston, long piston, froth and annular in his experiments. From his description and sketch, simple bubble and granular-lumpy bubble are bubble flow and the other, except annular, are intermittent flow. In the flow map reported by Barnea et al. the flow patterns were classed as dispersed bubble, elongated bubble, slug, churn and annular. They grouped

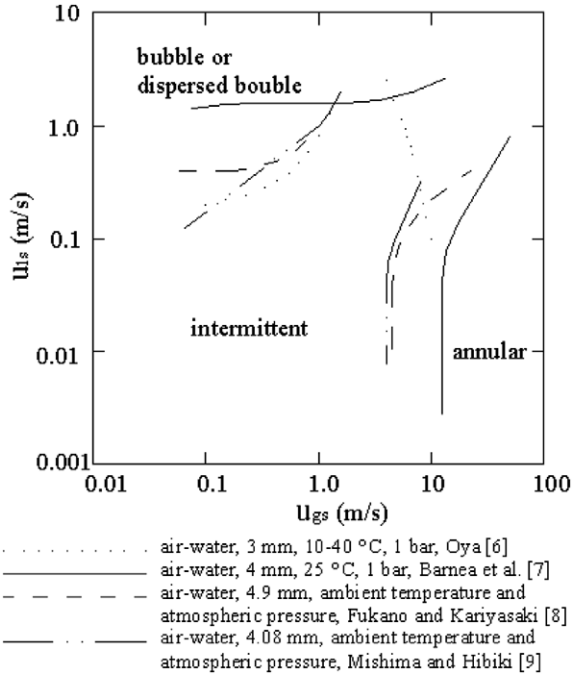

Fig. 1. Comparison of the air–water vertical upward flow maps at room condition.

elongated bubble, slug and churn as intermittent flow. Mishima and Hibiki's classification is similar to that of Barnea et al. They used bubbly flow instead of the dispersed flow and elongated bubble in Barnea et al., Fukano and Kariyasaki described only three flow patterns: dispersed bubble, intermittent and annular flow. Therefore, the experimental results can hardly be recognized or compared since there is no accepted benchmark among these researchers.

The factors affecting flow patterns are numerous and complex. In addition, the identification of flow patterns maybe greatly affected by the observer's subjectivity and the experimental technique employed. The transition from one flow pattern to another may be abrupt but in most cases it is a gradual development process in which case the transition boundary becomes a transition zone. Within the transition zone the flow patterns possess characteristics of more than one of the flow patterns. Although there are arguments on the classification of flow patterns, most researchers agreed to categorise flow patterns into four main classes: stratified flow, intermittent flow, annular flow and bubble flow. Each main class could be subdivided into subclasses. Table 2 lists the typical descriptions for two-phase flow patterns in normal and small tubes. Similar to normal size tubes, the observed flow patterns in small tubes in the earlier studies could be placed in the above-mentioned four main classes. However, on close observation, the flow patterns in small tubes exhibit different characteristics. For example, comparing with normal size tubes, stratified smooth flow is hardly observed in small channels whilst confined bubble flow emerges gradually in small channels due to the enhanced effect of surface tension. There is also a "problematic" region near intermittent and annular flow in small tubes. In this region the flow was observed as either wavy annular [7,10] or pseudo-slug [11], depending on the observers.

Although significant progress has been achieved and numerous results are now available, the theoretical study on small channel flow patterns is still at an early stage. No general model or correlation for small channels is validated or accepted widely. Some researchers tried to predict flow patterns in small tubes by the models deduced from

Table 2
Classification and description of flow patterns

Main class	Subclass for normal tubes	Subclass for small tubes
Stratified flow	Stratified smooth Stratified wavy	Stratified wavy
Bubble flow	Bubbly Dispersed bubble	Bubbly Dispersed bubble
Intermittent flow	Plug	Plug (confined bubble or elongated bubble)
	Slug (Taylor bubble)	Slug (Taylor bubble)
	Churn	Churn Pseudo-slug (wavy annular)
Annular flow	Annular Mist Wispy annular	Annular Mist

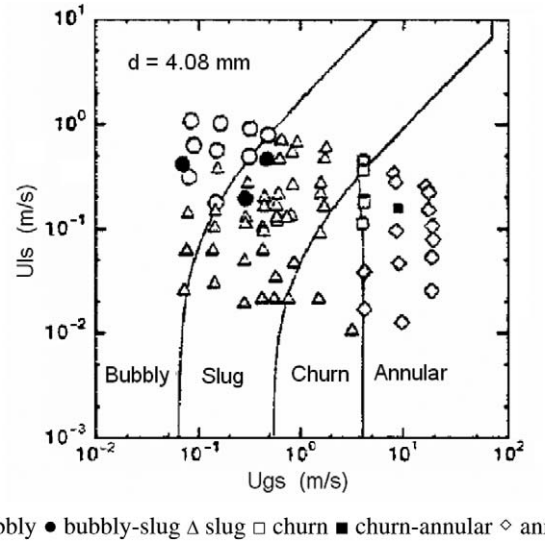

Fig. 2. Comparison by Mishima and Hibiki [9] of their experimental results for upward vertical flow with the model of Mishima-Ishii [12].

normal size tubes and reported good agreement. Mishima and Hibiki [9] sketched air–water flow maps for 1–4 mm vertical tubes at atmospheric conditions based on their experiments. They found that the transition boundaries were predicted well by the Mishima-Ishii's model [12], as seen in Fig. 2. However, most researchers came to a different conclusion because the existing models for normal channels ignore the effect of surface tension. Therefore, any such comparison lacks theoretical foundation [11,10,3]. Fig. 3 is a comparative plot of the experimental results of Damianides and Westwater [11] for air–water in a 1 mm internal diameter tube with the models presented

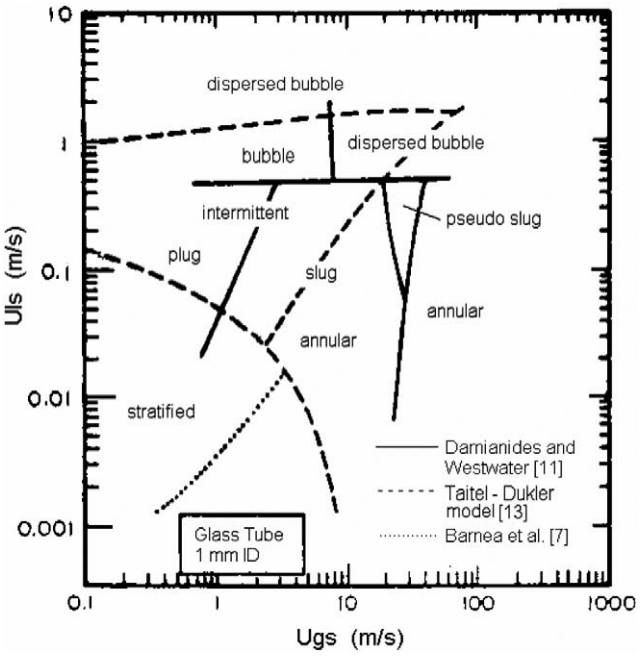

Fig. 3. Comparison between the 1 mm horizontal air–water flow map at atmospheric condition from Damianides and Westwater [11] and the models from Taitel and Dukler [13] and Barnea et al. [7].

in Taitel and Dukler [13] and Barnea et al. [7]. The figure shows clearly that not only the stratified flow did not appear in the 1 mm horizontal tube but also all transition boundaries cannot be predicted properly by the Taitel–Dukler model [13] and the Taitel modified model [7].

In traditional flow maps the transition boundaries are identified based on the gas–liquid interface configuration. However, a few flow regimes for small tubes as well as in experiments in microgravity were depicted based on force analysis in recent reports. Akbar et al. [4] divided the entire flow map for small tubes into four regions: (1) surface tension-dominated region, which included bubbly, plug and slug; (2) inertia-dominated zone 1, which included annular and wavy-annular regimes; (3) inertia-dominated zone 2, for the dispersed flow regime; (4) transition zone. They proposed semi-experimental correlations for regime predictions based on the above criteria and the previous experimental data in small channels, see Table 3. The correlations use the Weber number, $We_{ls} = \rho_l u_{ls}^2 D/\sigma$ and $We_{gs} = \rho_g u_{gs}^2 D/\sigma$, see also nomenclature, as the reference parameter which represents the ratio of surface tension and inertial force. The sketched transition boundaries agreed with the relevant data for air–water like fluid in circular and near-circular small tubes with ~1 mm hydraulic diameter at room conditions except the data of Mishima et al. [14]. The results are compared in Fig. 4. The authors suggested that the general applicability of the correlation needed further validation.

Table 3
The semi-experiential correlations for small tubes [4]

Flow regime	Conditions and equations
Surface tension dominated zone	$We_{gs} \leqslant 0.11 We_{ls}^{0.315}$ ($We_{ls} \leqslant 3.0$)
	$We_{gs} \leqslant 1.0$ ($We_{ls} > 3.0$)
Inertia dominated zone 1	$We_{gs} \geqslant 11.0 We_{ls}^{0.14}$
(annular flow zone)	$We_{ls} \leqslant 3.0$
Inertia dominated zone 2	$We_{gs} > 1.0$
(froth-dispersed flow zone)	$We_{ls} > 3.0$

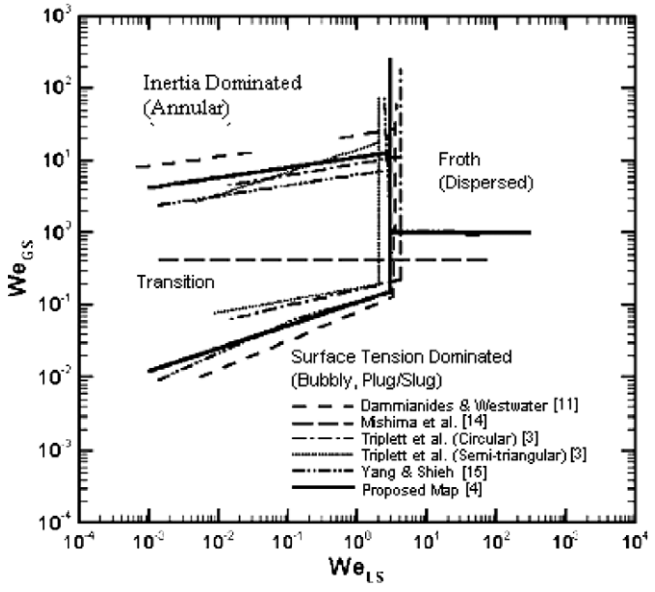

Fig. 4. The comparison between the correlations proposed by Akbar et al. [4] and the experimental data for circular and near-circular channels with ~1 mm diameter. See also Refs. [3,4,11,14,15].

The actual effect of diameter on the flow regimes is also a current topic of debate. Theoretically, flow patterns are less affected by channel orientation in small channels due to the relatively reduced effect of gravity as compared with large tubes. Therefore, the effect of channel dimension on the transition boundaries should be similar whether in vertical or in horizontal flow. However, researchers could not reach agreement on it. Damianides and Westwater [11] studied the flow regimes using air–water in horizontal tubes for the range of inside diameters 1, 2, 3, 4 and 5 mm. They reported that surface tension becomes a very important factor when the tube diameter is less than 5 mm at the experimental conditions (10–25 °C and atmospheric pressure). Some common tendencies of the transition boundaries were discovered in their studies. For instance, the intermittent-dispersed bubble transition boundary moves to the region of lower liquid flow rate with decreasing tube diameter; the intermittent-annular transition boundary moves to regions of higher gas flow rate with decreasing tube diameter, the stratified flow region gradually shrinks with decreasing tube diameter until it vanishes completely in the 1 mm tube. However, Coleman and Garimella [10] reported opposite trends. They too studied air–water in horizontal tubes of diameters 1.3, 1.75, 2.6 and 5.5 mm at atmospheric conditions. The results show clearly that the tube diameter has a significant effect on the transition boundaries. For example, the transition boundary of intermittent to dispersed bubble flow changes significantly as the tube diameter changes from 5.50 to 1.30 mm. However, the tendency of intermittent-dispersed bubble boundary to move to higher liquid flow rates with decreasing diameter contradicts the results of Damianides and Westwater [11]. For vertical tubes similar disagreements were reported. For example, Lin et al. [16] studied air–water flow patterns in 0.5–4.0 mm diameter tubes at the condition of 20 °C and 1 bar. They observed that the transition boundaries for slug to churn and churn to annular shift towards the region of lower gas flow rate as the tube diameter decreases. However, contradictory conclusions were reported by Zhao and Bi [17]. They experimentally investigated the characteristics of co-current upward air–water two-phase flow patterns in vertical equilateral triangular channels with hydraulic diameters of 2.886, 1.443 and 0.866 mm. They reported that dispersed bubbly flow shifted to higher liquid superficial velocity whilst churn and annular flow occurred at higher gas superficial velocity as the channel size was reduced. This tendency contradicts completely that reported by Lin et al. [16]. The results described above are summarized in Table 4.

In this study, accurate flow visualization experiments on adiabatic R134a flow patterns in small tubes were carried out. The main objectives of the work include: (i) obtain flow pattern maps, (ii) identify the critical diameter at the current experimental conditions, (iii) compare flow patterns with existing models and (iv) verify the effect of tube

Table 4
The direction of boundary shift with reducing channel dimensions

Researcher	Orientation	Diameter (mm)	Fluid	Intermittent/dispersed	Intermittent/annular	Stratified flow
Damianides and Westwater [11]	Horizontal	1, 2, 3, 4, 5	Air–water	Lower u_{ls}	Higher u_{gs}	Lower u_{gs} lower u_{ls}
Coleman and Garimella [10]	Horizontal	1.3, 1.75, 2.6, 5.5	Air–water	Higher u_{ls}	Higher u_{gs}	Lower u_{gs} lower u_{ls}
				To dispersed bubble	Slug/churn	To annular
Lin et al. [16]	Vertical	0.5–4	Air–water		Lower u_{gs}	Lower u_{gs}
Zhao and Bi [17]	Vertical	0.87, 1.44, 2.89	Air–water	Higher u_{ls}	Higher u_{gs}	Higher u_{gs}

Intermittent flow: plug or slug for horizontal tube and bubbly or slug for vertical tube.

diameter on flow patterns. Four different size tubes were studies, 1.10, 2.01, 2.88 and 4.26 mm which are expected to cover the range from normal to small size tubes.

2. Experimental facility

The experimental facility comprises three parts, i.e. the R22 cooling system, the R134a experimental system, and the control and data acquisition system. Fig. 5 shows the R134a experimental system. The facility is made of stainless steel, which is also suitable for a wide range of fluids including water. The liquid and vapour superficial velocity of R134a can reach 5 and 10 m/s, respectively. Details of the experimental system can be found in Chen et al. [18].

Four test sections, see Fig. 6, with internal diameter of 1.10, 2.01, 2.88 and 4.26 mm were examined. A test section is composed of a calming section, a heating section and an observation section. Fully-developed single-phase liquid flow is formed in the calming section. Two-phase flow is created by supplying electric current directly onto the thin-wall steal tube – the heating section. The observation section, a Pyrex glass tube with the same internal diameter as the steel heating tube, is directly connected to the outlet of the heating section. Flow patterns were observed and recorded by a high-speed digital camera (Phantom V4 B/W, 512×512 pixels resolution, 1000 pictures/s with full resolution and maximum 32,000 pictures/s with reduced resolution, minimum 10 μs exposure time).

The vital measurements in the flow pattern experiments are the temperatures ($T3$), the pressures ($P3$, $P4$, $P0$), the flow rate ($F1$ or $F2$) and the heating power (DPM2) in the test section, see Figs. 5 and 6. The thermocouple T3 uses the water triple point as a reference so as to improve the measuring accuracy. The same experimental facility was used for a parallel heat transfer study [19]. Hence more thermocouples were included in the rig and test section, e.g.

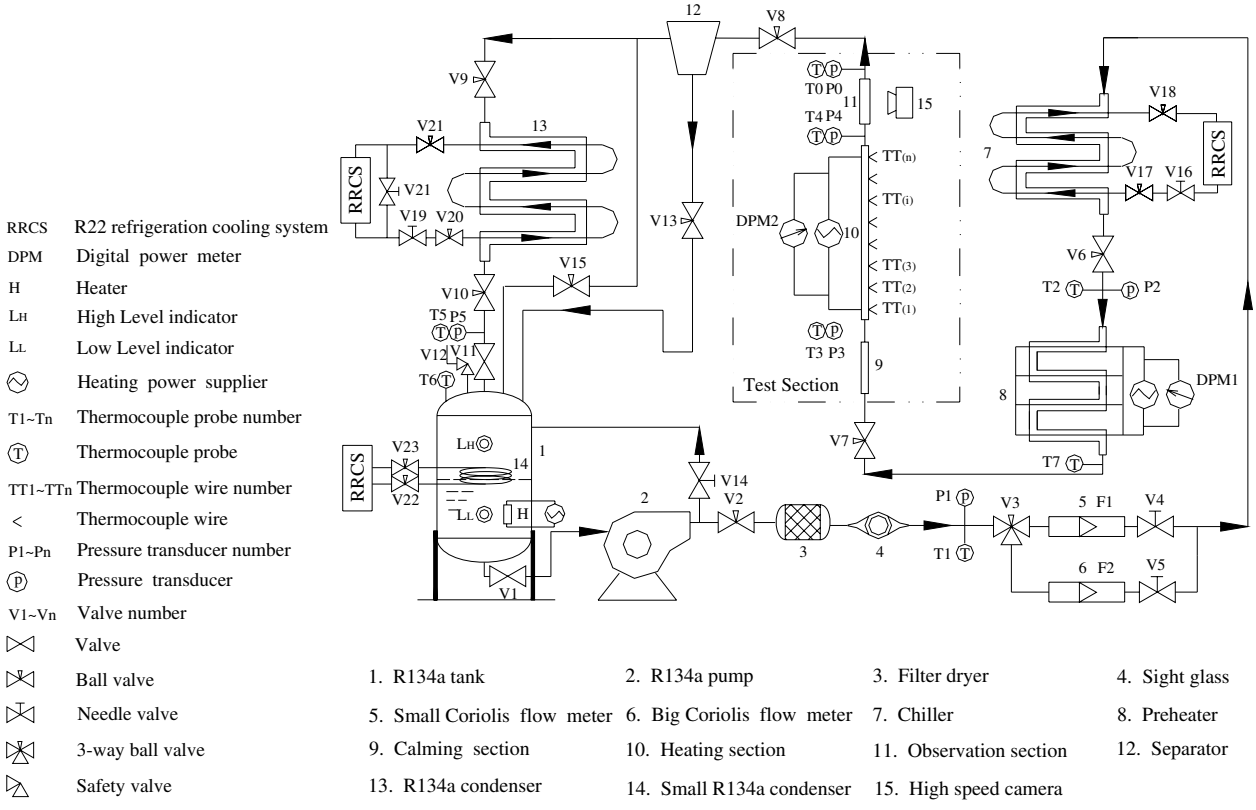

Fig. 5. Schematic diagram of the flow patterns experimental system (the R22 cooling system is not shown).

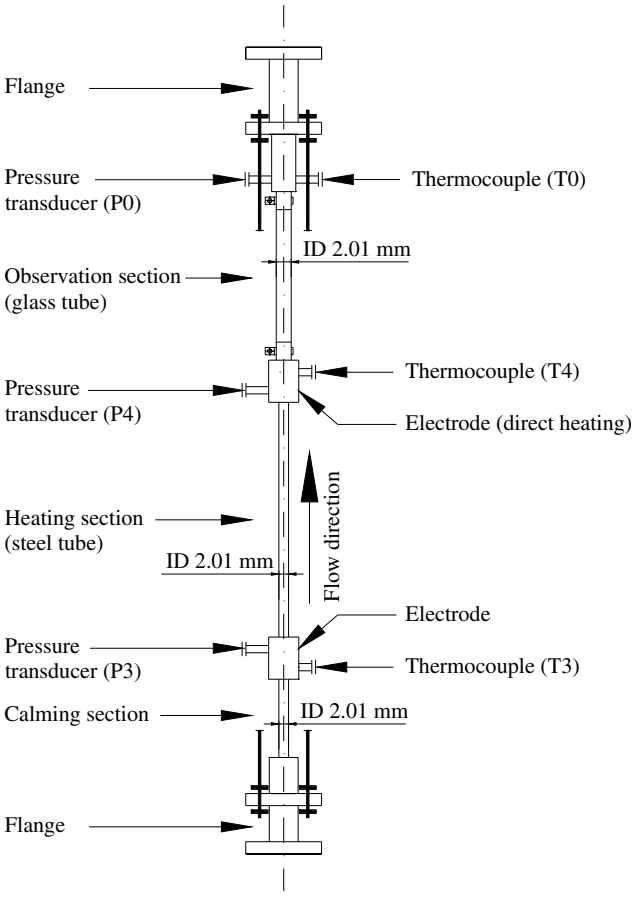

Fig. 6. Schematic diagram of the 2.01 mm test section.

$TT_{(1)} - TT_{(n)}$. In the present study they were used to estimate the heat loss and verify the condition at point 4, see Fig. 5. This data was also used to estimate the heat loss in the observation section. The system pressure is controlled through a heater in the R134a tank. The heater power is automatically adjusted by a PID controller based on the signal of the pressure at the exit of the observation section ($P0$).

All the instruments were carefully calibrated. Table 5 summarizes the uncertainties of the key parameters in the current experiments. The overall system performance was validated through single-phase experiments, e.g. the turbulent experimental friction factor agreed with the Blasius equation within ±5% over the Reynolds range of 4000–110,000. The experimental parameters at the observation point in the two-phase flow patterns experiments were deduced from the inlet and outlet saturated pressures and the assumption that the pressure drop along the observation section was linear. The liquid and vapour superficial velocities were varied and calculated for each diameter and pressure by changing the flow rate and heating power, see [18]. The number of data points near the transition boundaries was higher than that at other conditions in order to get more details at that zone. All the recorded data were taken at steady state conditions. This was verified by plotting the temperature and pressure at the inlet and exit of the test section against time and ensuring that they were steady.

Table 5
Summary of the uncertainty of the key experimental parameters

Item		Measurement range	Uncertainty range
Heating section (stainless steel tube)	1.10 mm ID tube		1.31%
	2.01 mm ID tube		0.59%
	2.88 mm ID tube		0.38%
	4.26 mm ID tube		0.26%
Observation section (glass tube)	1.10 mm ID tube		0.36%
	2.01 mm ID tube		0.17%
	2.88 mm ID tube		0.06%
	4.26 mm ID tube		0.11%
Pressure	$P3$	6–14 bar	0.42%
	$P4$	6–14 bar	0.26%
	$P0$	6–14 bar	0.26%
Temperature	$T3$, $T4$, $T0$	20–55 °C	0.16 K
	TT1 − TT15	>20 °C	0.16 K
Flow rate	Small meter CMF010	0.5–25 kg/h	0.15–0.54%
	Large meter CMF025	25–500 kg/h	0.15–0.22%
Heating power	Test section	2.68–1640 W	0.10–0.49%
Differential pressure	24% full scale	0–0.0608 bar	21.16 Pa
	100% full scale	0.0608–0.2491 bar	77.43 Pa
Quality (absolute error)	1.10 mm test section	0–100%	0.14–1.37%
	2.01 mm test section	0–100%	0.14–2.88%
	2.88 mm test section	0–100%	0.14–3.33%
	4.26 mm test section	0–100%	0.14–3.21%
Gas superficial velocity	1.10 mm	0.01–10 m/s	0.011–0.41 m/s
	2.01 mm	0.01–10 m/s	0.006–0.34 m/s
	2.88 mm	0.01–10 m/s	0.004–0.32 m/s
	4.26 mm	0.01–10 m/s	0.002–0.32 m/s
Liquid superficial velocity	1.10 mm	0.04–5 m/s	0.0009–0.15 m/s
	2.01 mm	0.04–5 m/s	0.0003–0.07 m/s
	2.88 mm	0.04–5 m/s	0.0002–0.05 m/s
	4.26 mm	0.04–5 m/s	0.0001–0.03 m/s

3. Experimental results

Dispersed bubble, bubbly, slug, churn and annular flow were observed in all four test sections. Occasionally mist flow was observed in the bigger tubes at very high vapour velocity whilst confined bubble flow was found in smaller tubes at lower vapour and liquid velocity. The above-mentioned seven flow patterns are defined as follows:

Dispersed bubble: numerous small bubbles float in a continuous liquid phase.

Bubbly: bubble size is comparable to but not as large as the tube diameter.
Confined bubble: bubble size reaches the diameter of the tube and is confined by the tube wall. They have regular vapour-liquid interface and spherical cap and bottom.
Slug: bubbles develop into bullet shape due to the tube wall restriction. Sometimes the bullet bubble is followed by a stream of small bubbles creating a trail.
Churn: bullet bubbles start to distort and small bubbles in liquid slug coalesce into gas clump with increase of gas velocity – a highly oscillatory flow with chaotic interface.
Annular: gas phase becomes a continuous flow in the core of tube.
Mist: liquid film is blown away from tube wall and numerous liquid droplets float in high-speed vapour flow.

Figs. 7–10 show the above flow patterns at 10 bar pressure. The flow patterns in 2.01 and 4.26 were first reported in Chen et al. [18] but are included here for completeness. Overall the flow patterns in the four tubes are similar and could be grouped into the above seven typical patterns – note that pure mist flow was obtained in the 4.26 mm tube only. Annular-mist transition flow was observed in the 2.01, 2.88 and 4.26 mm tubes, i.e. liquid film sticks on the tube wall whilst the liquid droplets pass through intermittently. This discontinuous liquid droplet flow may be the result of the collapse of liquid slug in churn flow in the heating section. The high velocity vapour current breaks up the liquid bridges and creates numerous liquid droplets. After that, the experiments were stopped in the 2.01 and 2.88 mm tubes before reaching critical heat flux. The 1.10 mm tube was not tested under very high fluid velocity because the resulting excessive pressure drop caused system unsteadiness. Similar results were obtained at the 6 and 14 bar pressures. As stated before, all the flow patterns observed in the four tubes could be categorized in the above typical regimes. However, on close observation, there are some differences among these tubes. Confined bubble flow, similar to slug flow but with elongated spherical top and bottom bubbles, was only observed in the 1.10 mm tube at 6.0–14.0 bar and the 2.01 mm tube at 6.0 bar. It indicates that surface tension was grown into the dominant force in the smaller tubes at the lower fluid velocities. With the increase of fluid velocities, as shown in Fig. 7, the gas–liquid interface became irregular and chaotic. Inertial force and friction gradually replace surface tension to become the important factors in flow pattern transition.

The flow patterns in the 2.88 and 4.26 mm tubes do not exhibit any common characteristics of the flow patterns in small tubes. Comparatively, the flow patterns in the 2.01 mm tube show some ‘‘small tube characteristics’’,

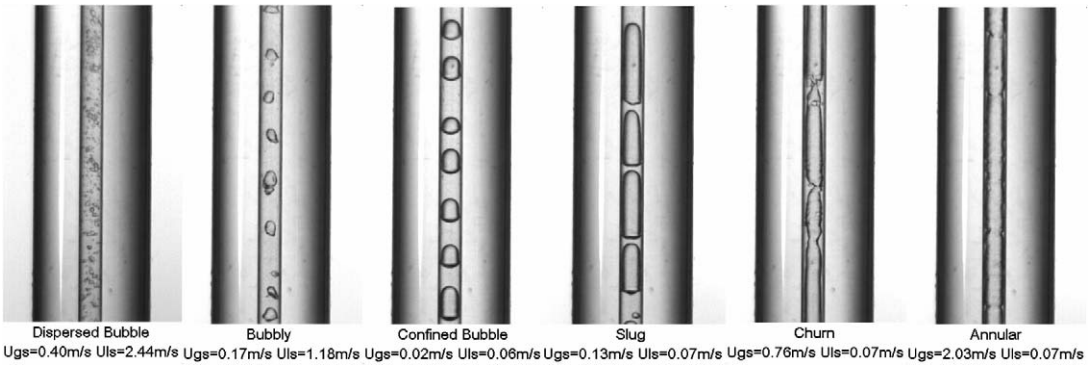

Fig. 7. Flow patterns observed in the 1.10 mm internal diameter tube at 10 bar.

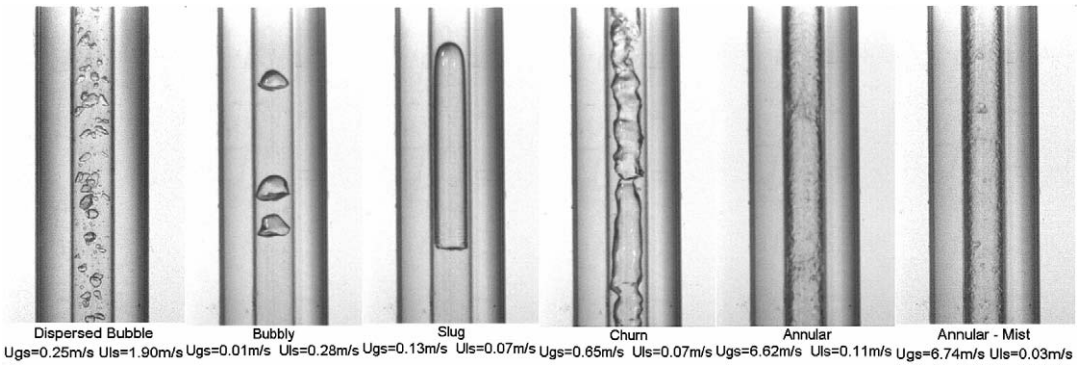

Fig. 8. Flow patterns observed in the 2.01 mm internal diameter tube at 10 bar.

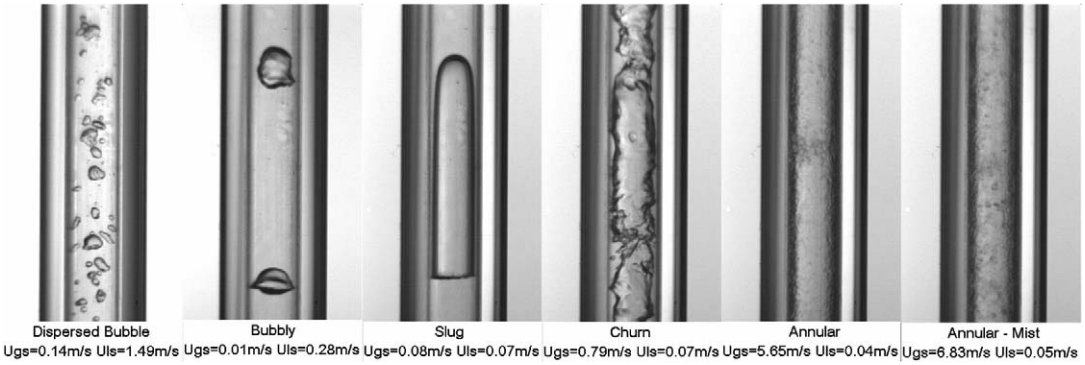

Fig. 9. Flow patterns observed in the 2.88 mm internal diameter tube at 10 bar.

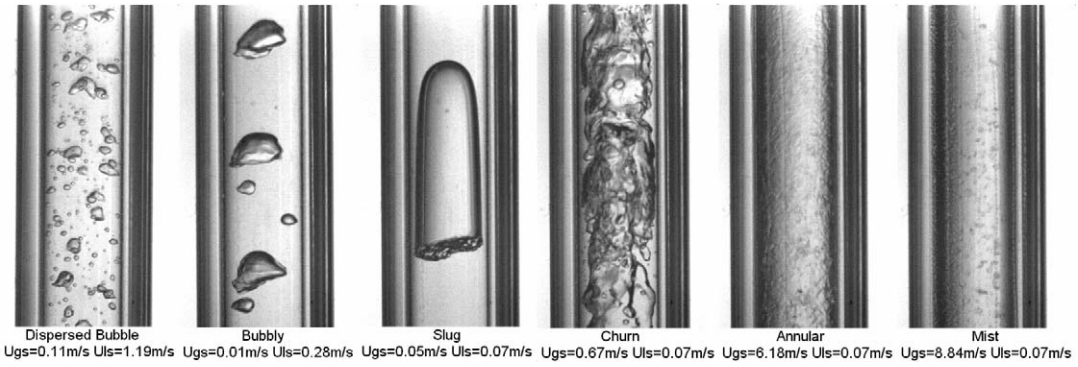

Fig. 10. Flow patterns observed in the 4.26 mm internal diameter tube at 10 bar.

which indicates the increasing action of surface tension and tube confinement, e.g. the appearance of the confined bubble flow, the slimmer vapour slug, the thinner liquid film around the vapour slug, and the less chaotic vapour–liquid interface in churn flow. When tube diameter decreases to 1.10 mm, the full small tube characteristics, as also described in the previous studies [6,11,8,9,3,16], are exhibited. Therefore, the 2.01 mm tube possesses both characteristics of normal size and small size tube. From this point of view, a tube diameter around 2.0 mm can be regarded as the critical diameter for refrigerant R134a at the current experimental conditions. This result agrees with the criterion by Kew and Cornwell [1], e.g. 1.7–1.4 mm at 6–14 bar.

Twelve flow pattern maps were generated based on all the results obtained for the 1.10, 2.01, 2.88 and 4.26 mm tubes at 6, 10 and 14 bar pressure. The flow pattern maps for the 2.01 and 4.26 mm tubes were compared with the existing models for vertical upward flow in normal size tubes and showed poor agreement in Chen et al. [18]. The models included the unified model summarized by Taitel [20] and the models given by Taitel et al. [21], Mishima and Ishii [12] and McQuilian and Whalley [22]. Comparatively the unified model matched the experimental data better for the 4.26 mm tube than the other models. Therefore, Figs. 11–14 depict the comparison of the experimental flow maps for the 1.10–4.26 mm tubes with the unified model summarized by Taitel [20] to investigate its applicability for the smaller tubes. As expected, the newly obtained flow maps for the 1.10 and 2.88 mm tubes cannot be predicted by the models and the discrepancy is higher in the smaller tubes. For example, the shaded region in which the predicted annular flow falls into the region of slug flow increases and the disagreement on the transition boundary of dispersed bubble to slug flow between our data and the predictions increases as the diameter gets smaller.

The effect of diameter on flow pattern transition boundaries is depicted in Figs. 15 and 16. Reducing the diameter shifts the transition boundaries of slug-churn and churn-annular to higher vapour velocities. This result is in agreement with the experiments of Zhao and Bi [17], Coleman and Garimella [10] and Damianides and Westwater [11] but contrary to the results of Lin et al. [16]. Also, the dispersed bubble–bubbly boundary shifts to higher liquid velocity with a reduction in the diameter, which agrees with Zhao and Bi [17] and Coleman and Garimella [10] but is in disagreement with the report of Damianides and Westwater [11], see Table 4. There seems to be no change for these four diameters at the boundaries of dispersed bubble-churn and bubbly-slug flow. The trends are similar for $P = 10$ bar.

The suitability of number of different parameters (17 in total listed in Chen [23]), as coordinates in addition to the superficial velocities, were also examined in the present project. An interim conclusion reached is that the use of the Weber number may be a good choice, see Figs. 17 and 18. As seen in the figures, almost all transition boundaries,

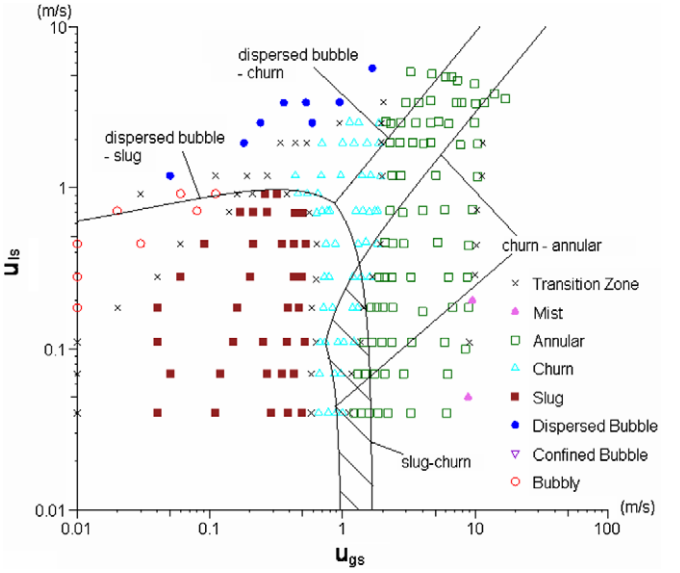

Fig. 11. Flow pattern map for R134a in the 4.26 mm tube at 10 bar and comparison with the unified model [20].

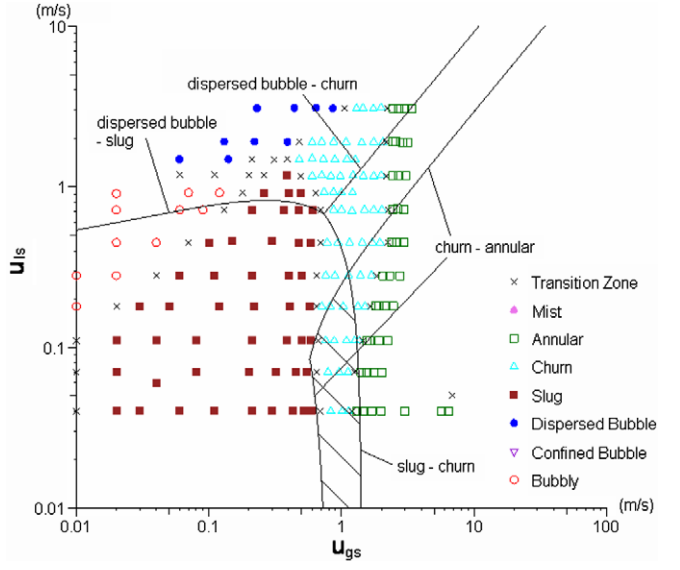

Fig. 12. Flow pattern map for R134a in the 2.88 mm tube at 10 bar and comparison with the unified model [20].

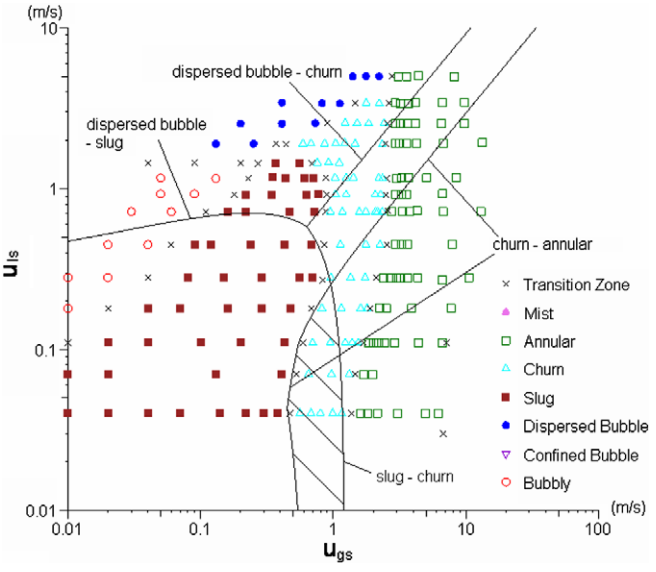

Fig. 13. Flow pattern map for R134a in the 2.01 mm tube at 10 bar and comparison with the unified model [20].

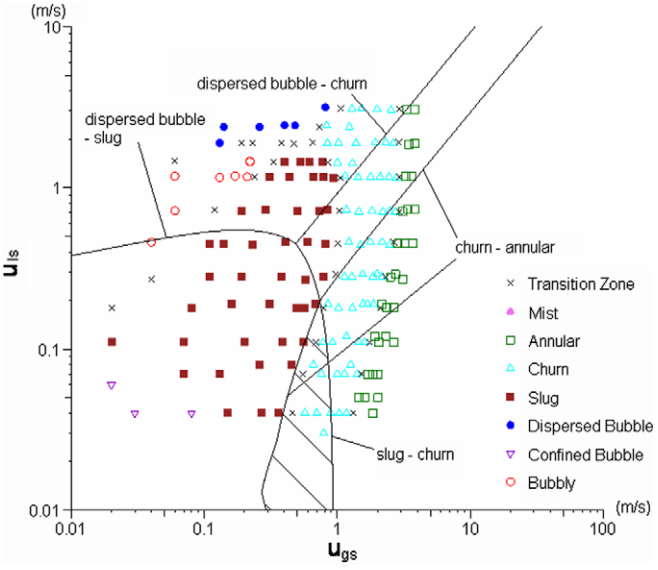

Fig. 14. Flow pattern map for R134a in the 1.10 mm tube at 10 bar and comparison with the unified model [20].

except bubble-dispersed bubble and slug-churn at the lower u_{ls} region, are superimposed. There seems to be a perfect match for these transition boundaries for all pressures. It seems to indicate that the effect of channel size is to a great extend correctly represented by the Weber number and may be useful in deducing the flow regimes for different size tubes from such maps. However, this needs further study and validation.

Fig. 19 compares the present experimental data at 10 bar and the semi-experimental correlation for small tubes [4]. Obviously the results show poor agreement. The transition boundaries predicted by the correlations (see Table 3) are sketched in solid lines and the current observed flow patterns are labelled in brackets. None of the flow patterns at the current experimental conditions are predicted well. The same conclusion was obtained when the experimental results for 6 and 14 bar were compared with the correlation of Akbar et al. The possible explanation to such discrepancy is (1) the proposed correlations were based on the experimental data using air–water in horizontal tubes, (2) Akbar et al. suggested $Bo = 0.3$ as the criterion to define a small tube, i.e. the corresponding critical diameter is less than 0.25 mm at the present experimental conditions, see Table 1. Therefore, the correlations proposed by Akbar et al. [4] may not be applicable in this case. The development of a general set of correlation equations needed to cover the range of small to microdiameters calls for further research work.

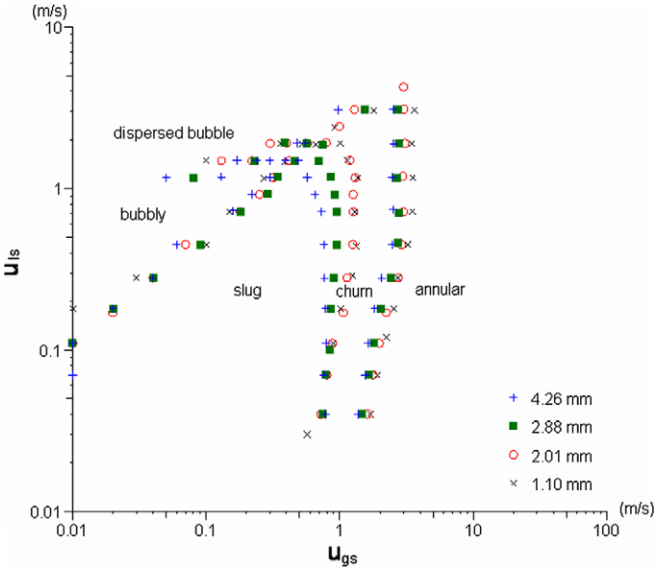

Fig. 15. Effect of diameter on transition boundaries at 6 bar.

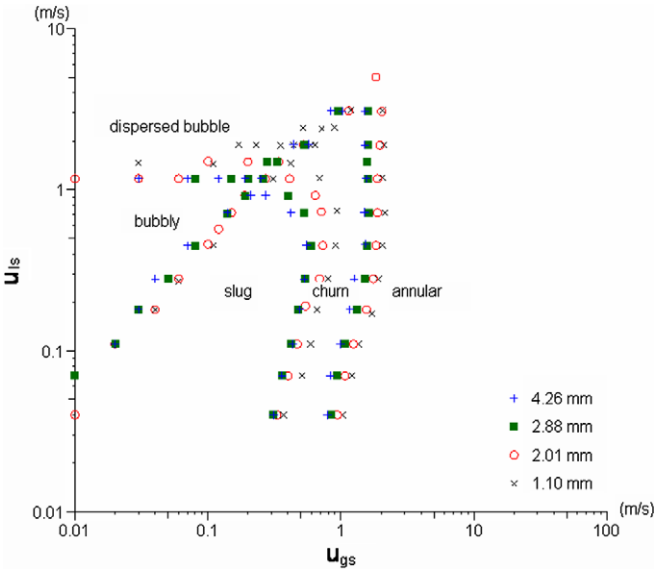

Fig. 16. Effect of diameter on transition boundaries at 14 bar.

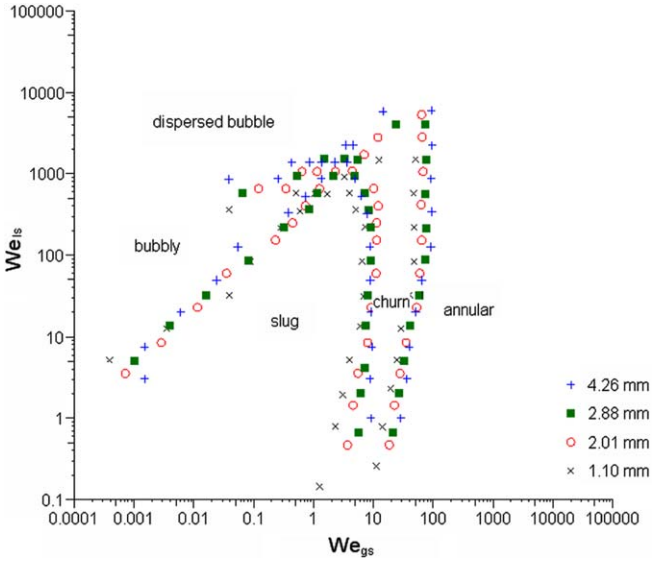

Fig. 17. R134a flow map in *We* coordinate system at 6 bar.

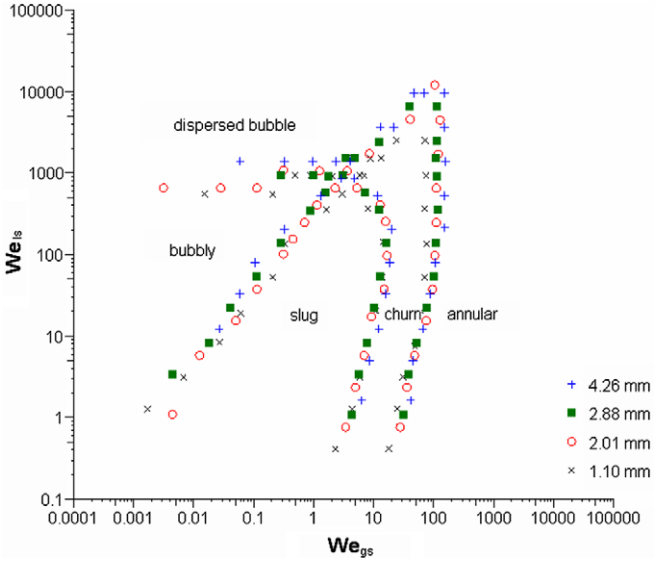

Fig. 18. R134a flow map in *We* coordinate system at 14 bar.

4. Conclusions

Seven typical flow patterns were observed in the present experimental conditions, i.e. dispersed bubble, bubbly, confined bubble, slug, churn, annular and mist. The experimental results indicate that the flow patterns for the larger diameters (2.88 and 4.26 mm) strongly resemble flow pattern characteristics found in normal size tubes. When the tube diameter was reduced to 2.01 mm, the flow patterns exhibit some "small tube characteristics" until the confined bubble flow appears in the 1.10 mm tube at all experimental pressures which indicates that surface tension became the dominant force. The critical diameter used to distinguish small and normal pipes could be deduced from the above observations and is about 2 mm for the current experimental conditions. Twelve flow pattern maps were drawn and compared with the existing models for normal size tubes indicating significant differences in the 4.26 mm tube and more so for the smaller tubes. The boundaries of slug to churn and churn to annular moved to higher vapour velocity whilst the dispersed bubble to bubbly boundary moved to higher liquid velocity when the diameter changed from 4.26 to 1.10 mm. The diameter does not seem to affect the dispersed bubble to churn and bubbly to slug. The current research and experimental data indicates that the Weber number may be the right parameter to deduce general correlations to predict the transition boundaries that include the effect of diameter. This can form the basis or subject for further research in this area.

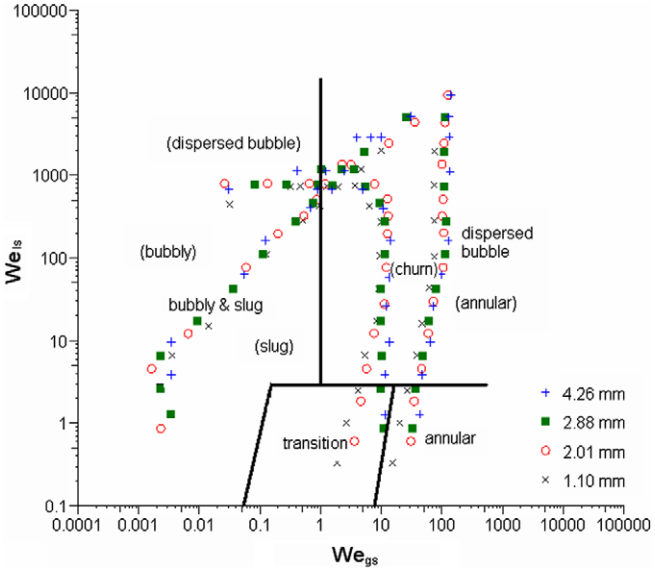

Fig. 19. The comparison between the correlations proposed by Akbar et al. [4] and the present experimental data at 10 bar.

References

[1] P.A. Kew, K. Cornwell, Correlations for the prediction of boiling heat transfer in small-diameter channels, Appl. Therm. Eng. 17 (8–10) (1997) 705–715.

[2] N. Brauner, D. Moalem-Maron, Identification of the range of small diameter conduits, regarding two-phase flow pattern transitions, Int. Commun. Heat Mass Transfer 19 (1992) 29–39.

[3] K.A. Triplett, S.M. Ghiaasiaan, S.I. Abdel-Khalik, D.L. Sadowski, Gas–liquid two-phase flow in microchannels, Part I: Two-phase flow patterns, Int. J. Multiphase Flow 25 (1999) 377–394.

[4] M.K. Akbar, D.A. Plummer, S.M. Ghiaasiaan, On gas–liquid two-phase flow regimes in microchannels, Int. J. Multiphase Flow 29 (2003) 855–865.

[5] S.G. Kandlikav, Fundamental issues related to flow boiling in minichannels and microchannels, Exp. Therm. Fluid Sci. 26 (2002) 389–407.

[6] T. Oya, Upward liquid flow in small tube into which air streams (1st report, Experimental apparatus and flow patterns), vol. 14, no. 78, 1971, pp. 1320–1329.

[7] D. Barnea, Y. Luninski, Y. Taitel, Flow pattern in horizontal and vertical two phase flow in small diameter pipes, Can. J. Chem. Eng. 61 (5) (1983) 617–620.

[8] T. Fukano, A. Kariyasaki, Characteristics of gas–liquid two-phase flow in a capillary tube, Nucl. Eng. Des. 141 (1993) 59–68.

[9] K. Mishima, T. Hibiki, Some characteristics of air–water two-phase flow in small diameter vertical tubes, Int. J. Multiphase flow 22 (4) (1996) 703–712.

[10] J.W. Coleman, S. Garimella, Characterization of two-phase flow patterns in small diameter round and rectangular tubes, Int. J. Heat Mass Transfer 42 (1999) 2869–2881.

[11] D.A. Damianides, J.W. Westwater, Two-phase flow patterns in a compact heat exchanger and in small tubes, in: Second UK National Conference on Heat Transfer, vol. 11 Sessions 4A–6C, 1988, pp. 1257–1268.

[12] K. Mishima, M. Ishii, Flow regime transition criteria for upward two-phase flow in vertical tubes, Int. J. Heat Mass Transfer 27 (5) (1984) 723–737.

[13] Y. Taitel, A.E. Dukler, A model for predicting flow regime transitions in horizontal and near-horizontal flow, AIChE 22 (1976) 47–55.

[14] K. Mishima, T. Hibiki, H. Nishihara, Some characteristics of air–water two-phase flow in small diameter tubes, in: Proceedings of the 2nd International Conference Multiphase Flow, vol. 4, April 3–7, Tokyo, Japan, 1995, pp. 39–46.

[15] C.Y. Yang, C.C. Shieh, Flow pattern of air–water and two-phase R-134a in small circular tubes, Int. J. Multiphase Flow 27 (2001) 1163–1177.

[16] S. Lin, P.A. Kew, K. Cornwell, Two-phase flow regimes and heat transfer in small tubes and channels, in: Heat Transfer1998, Proceedings of 11th IHTC, vol. 2, August 23–28, Kyongju, Korea, 1998, pp. 450–500.

[17] T.S. Zhao, Q.C. Bi, Co-current air–water two-phase flow patterns invertical triangular microchannels, Int. J. Multiphase Flow 27 (2001) 765–782.

[18] L. Chen, Y.S. Tian, T.G. Karayiannis, R134a Flow patterns in small diameter tubes, J. Process Mech. Eng., Proc. Inst. of Mech. Engrs., Part E 219 (2005) 167–181.

[19] X. Huo, Y.S. Tian, T.G. Karayiannis, R134a flow boiling heat transfer in small diameter tubes, Int. J. Heat Exchangers, in press.

[20] Y. Taitel, Flow pattern transition in two phase flow, Keynote lecture, in: 9th International Heat Transfer Conference, Jerusalem, Israel, 19–24 August, 1990, pp. 237–254.

[21] Y. Taitel, D. Barnea, A.E. Dukler, Modelling flow pattern transitions for steady upward gas–liquid flow in vertical tubes, AIChE 26 (1980) 345–354.

[22] K.W. McQuillan, P.B. Whalley, Flow patterns in vertical two-phase flow, Int. J. Multiphase Flow 11 (2) (1985) 161–175.

[23] L. Chen, Flow patterns in upward two-phase flow in small diameter tubes, Ph.D. thesis, Burnel University, UK, submitted.